Lasers in Surgery and Medicine 27:158–164 (2000)

# Laser Irradiative Tissue Probed In Situ by Collagen 380-nm Fluorescence Imaging

Jing Tang, MD, PhD,[1] Fanan Zeng, MS,[1] Howard Savage, PhD,[2] Peng Pei Ho, PhD,[1] and R.R. Alfano, PhD[1]*

[1]Institute for Ultrafast Spectroscopy and Lasers and New York State Center for Advanced Technology for Ultrafast Photonic Materials and Applications, Departments of Electrical Engineering and Physics, The City College of the City University of New York, New York

[2]Department of Pathology, New York Eye and Ear Infirmary, New York, New York

***Background and Objective:*** **There is no ideal method to detect molecular changes in situ of laser-irradiated tissue without removing a section of tissue for histologic examination. A new method is reported to evaluate laser-induced thermal tissue damage in situ by using 380-nm native fluorescence imaging under 340-nm excitation.**

***Study Design/Materials and Methods:*** **Native fluorescence imaging was performed on laser irradiated bovine tendon tissue and compared with light illuminated photography and histology with picrosirius red F3BA stain.**

***Results and Conclusion:*** **The results indicate that a decrease in collagen fluorescence at 380 nm was observed in laser-induced thermally damaged tissues. The injured region of tissue defined by its fluorescence image coincided with an area defined by photography and histology.**

**Lasers Surg. Med. 27:158–164, 2000** 

**Key words: fluorescence imaging; tissue thermal damage; collagen; laser irradiative**

## INTRODUCTION

Laser based therapies such as photocoagulation and interstitial hypothermia [1], angioplasty and recanalization [2], and tissue welding [3–5] usually depend on heating the tissue target. When the photons are absorbed, the energy is transformed into heat by nonirradiative transition, causing the temperature to rise in the excitation region. The process can lead to protein dehydration, denaturation, coagulation, and/or ablation. These therapies depend on the delivery of well-defined thermal energy to a local region. To minimize the extent of thermal injury in the normal tissue area, a reliable method for detecting tissue thermal damage in situ is desirable.

Native fluorescence spectroscopy has the potential to monitor molecular changes and can be used to probe changes in tissues [6]. There are several natural fluorophores in tissue, such as collagen and elastin. Fluorescence spectral imaging offers a novel way to monitor tissue thermal damage in situ. Most recently, we have succeeded in detecting the changes in collagen and elastin levels after laser skin welding using native fluorescence imaging [7]. Collagen is one of the most abundant animal proteins in mammals, accounting for up to 30% of all proteins [8]. It occurs in most tissues, such as skin, tendon, bone, and cornea [9]. Changes in the collagen state by means of fluorescence spectroscopy offer a molecular marker.

This study focuses on the use of native fluorescence to monitor in situ laser-induced thermal tissue damage. White light illuminated photography and histology confirmed the changes monitored by fluorescence.

Contract grant sponsor: DOE Center of Excellence Program.

*Correspondence to: R.R. Alfano, Institute for Ultrafast Spectroscopy and Lasers, Department of Physics, The City College of the City University of New York, 138th Street and Convent Avenue, New York, NY 10031.

Accepted 27 March 2000

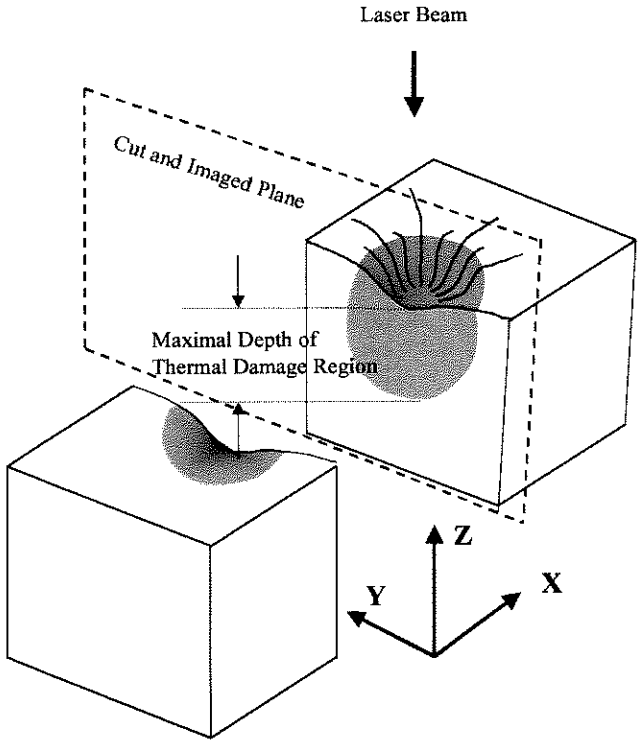


Fig. 1. Bovine tendon sample for photography and fluorescence imaging. After argon laser treatment, the tissue surface ($x$-$y$ plane) become distorted and deformed.

## MATERIALS AND METHODS

The powder of collagen type I (Sigma, St. Louis, MO) was used as a control and reference. It was situated in a 1-mm-thick quartz cuvette. The bovine tendon was purchased from a local market and considered as a homogeneous (on a macroscopic level) and collagen-rich biological test medium. The samples were cut as a 7 × 7 mm square with 5 mm in thickness. Argon laser irradiation was performed perpendicularly to the surface of the bovine tendon sample with duration of 3, 6, 9, 12, and 15 seconds, respectively (n = 6 for each time group). Then, the samples were mounted on a quartz slide for spectral analysis and back illuminated photography. After irradiation, the native fluorescence images and photographs were first measured for the $x$-$y$ plane surface as shown in Figure 1. The sample was kept at −20°C for 15 minutes. While the sample was frozen, a $y$-$z$ plane section through the maximum diameter of the lesion was made as shown in Figure 1. The native fluorescence images and photographs for the $y$-$z$ plane section of the sample were performed at room temperature. Spectroscopic measurements were performed by using an automated lamp-

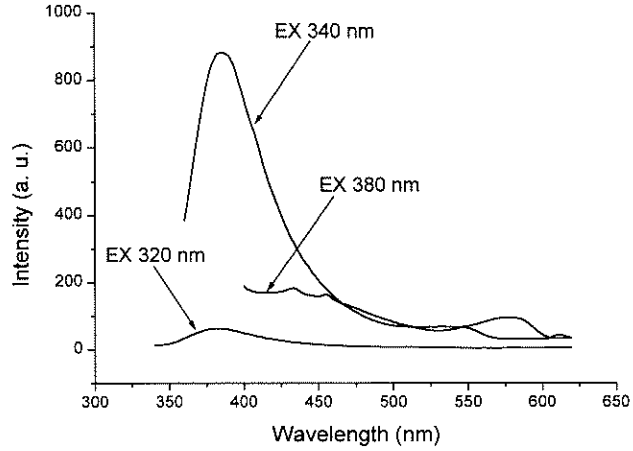


Fig. 2. Fluorescence spectra from collagen excited at different wavelengths [7].

based spectrophotometer, CD-scan from Mediscience Technology Corp. Imaging the fluorescence emission at 380-nm with 340-nm excitation was selected to study the collagen native fluorescence after thermal treatment. Fluorescence spectra of collagen with different excitation wavelengths from 320 to 380 nm are shown in Figure 2.

A schematic diagram of the 380-nm fluorescence imaging setup used is shown in Figure 3a. A light beam from a high-intensity xenon lamp (300 W) was passed through a broad band filter to cut a part of heat and then transmitted by an optical fiber (Excitation Fiber). Narrow band filters selected the excitation and emission wavelengths. Before exciting the surface of the sample, the light beam was passed through a 340-nm narrow band filter (Excitation Filter), with a 10-nm bandwidth. The final power density of excitation light on the sample surface was 35 $\mu W/cm^2$ measured by a multifunction optical meter (Newport, Model 1835-e, Irvine, CA). The fluorescence from the sample was collected by a 105-mm UV-Nikkor camera lens (UV Lens #1) in the back-scattering geometry and sent into an image intensifier. A 380-nm narrow band filter (Emission Filter) was inserted at the front of the Lens #1 to select a portion of the fluorescence. After the signal was amplified by an image intensifier, the fluorescence image was re-imaged with another lens (Lens #2) onto a CCD camera (TM-72EX, Pulnix America, Inc., Sunnyvale CA). Three frames in 1 second can be obtained from this imaging system. To improve the signal to noise, each image presented was averaged over 10 frames. A personal computer was used to digitize and analyze the

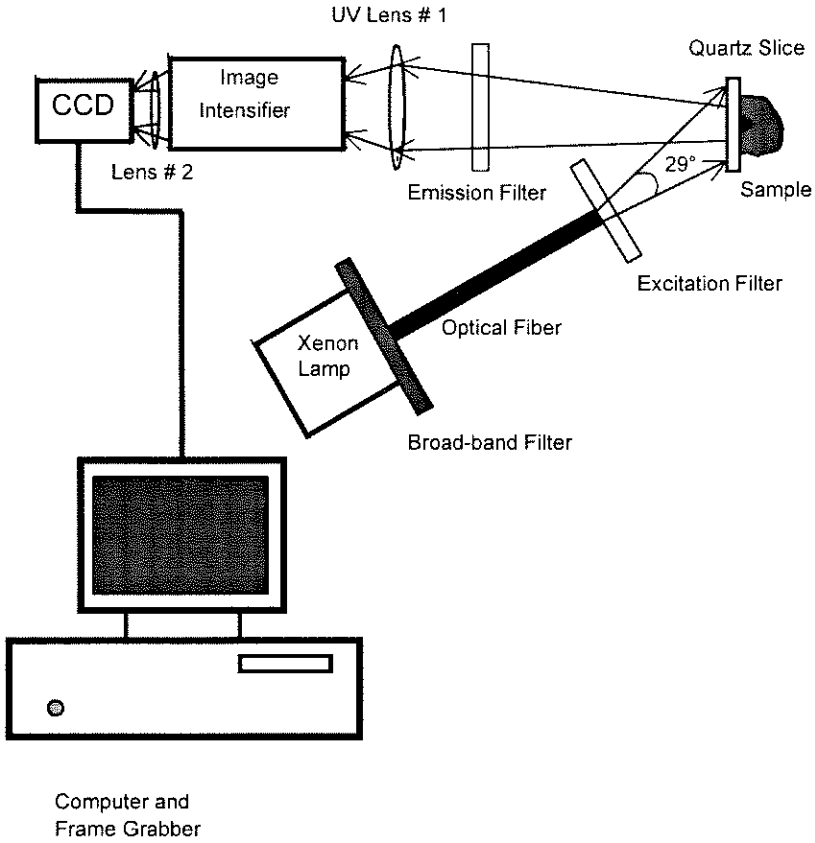


(a)

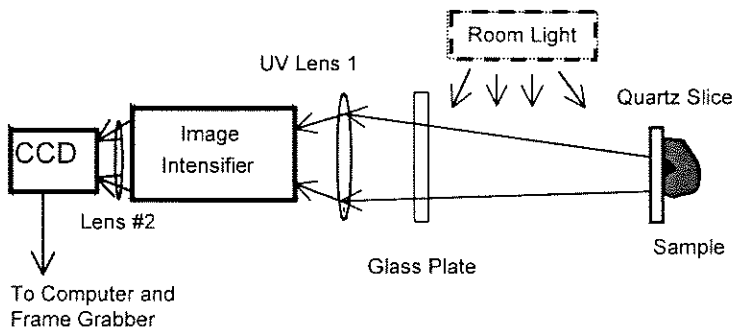


(b)

Fig. 3. Optical imaging setups. **a:** The setup for native fluorescence imaging to probe the thermal damage region. The light beam from the xenon lamp is sent through the broad-band filter and then transmitted by the Excitation Fiber. Before exciting the surface of the sample, the light beam is passed through the Excitation Filter (340 nm). The fluorescence from the sample is collected by UV Lens #1 and imaged onto an image intensifier. The Emission Filter (380 nm) is inserted at the front of the UV Lens #1 for fluorescence imaging. After the signal is amplified by the image intensifier, the fluorescence image is re-imaged with Lens #2 onto the CCD camera. The personal computer is used to digitize and analyze the image. **b:** White light illuminated photography setup. The glass plate is placed at the front of the UV Lens #1 instead of the emission filter to obtain the same focus as with fluorescence imaging. The sample is illuminated with room daylight.

image. The controlling software generated and displayed the fluorescence maps of the tissue.

For the white light illuminated photography setup (Fig. 3b), a glass plate was placed at the front of the Lens #1 instead of the emission filter to obtain the same focus and size image as for fluorescence imaging. The sample was illuminated with fluorescent lights from the ceiling.

The multiline visible argon laser beam (Model Innovar 400, Coherent, Santa Clara, CA) was used to produce thermal damage in the tissue. The laser beam was delivered in free space with noncontact. The beam was focused with a

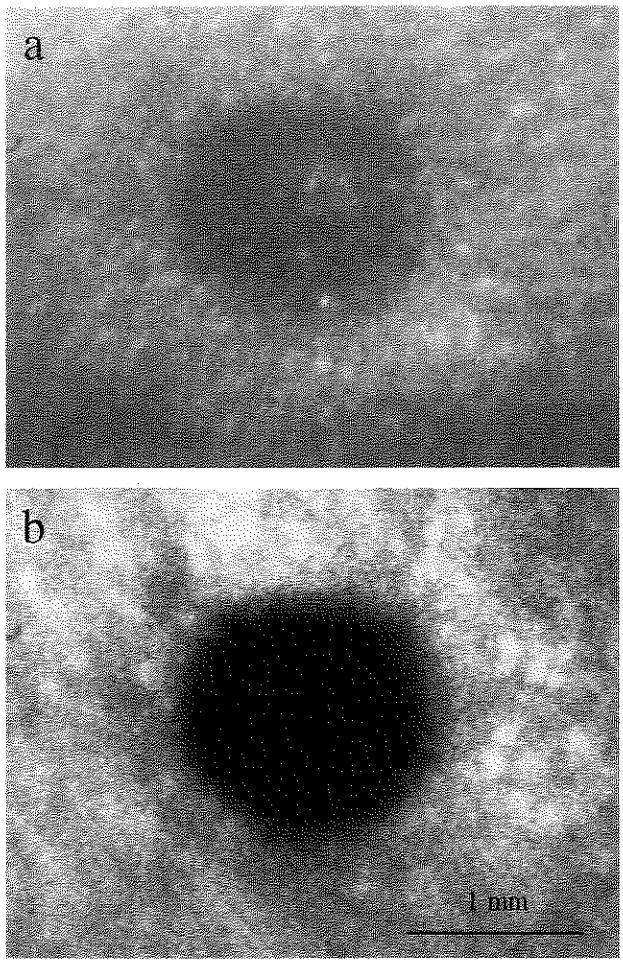


Fig. 4. The surface ($x$-$y$ plane) of a tendon tissue sample after irradiation by an argon laser. **a:** The thermal damage region detected with white light illuminated photography. **b:** The thermal damage region (dark part) on the same sample detected with native fluorescence imaging at an emission of 380 nm with an excitation at 340 nm. The thermal damage region is shown much more clearly in the fluorescence image than in white light photography.

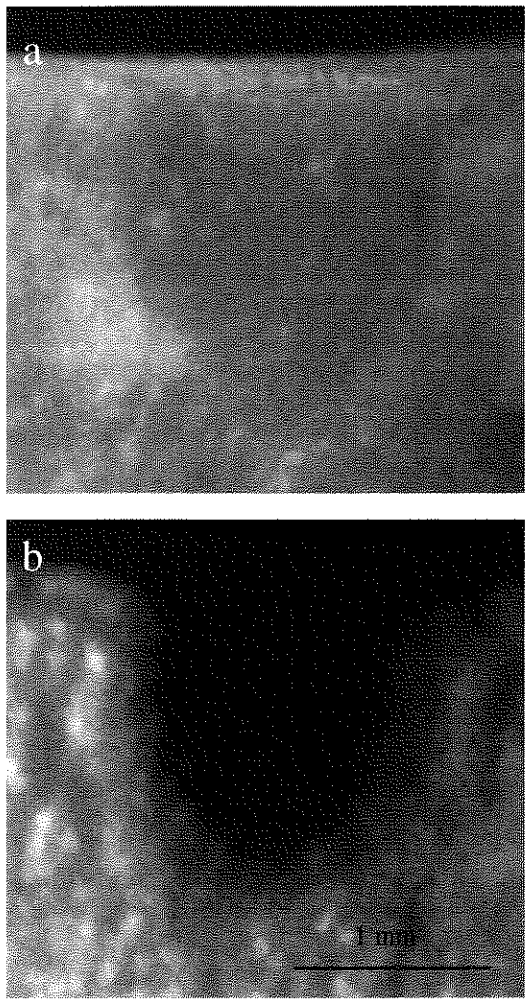


Fig. 5. The $y$-$z$ plane section of a tendon tissue sample after irradiation by an argon laser. **a:** The thermal damage region in the cross-section with light illuminated photography. **b:** The thermal damage region (dark part) on the same sample detected with native fluorescence imaging. The damage region is clearer in the fluorescence image than in the white light photography.

short focal length lens (f = 60 mm) producing a spot size of 1 mm. The sample was positioned at 50 mm from the lens. The laser output power was kept at 2.15 W measured with a power meter (Scientech 372, Boulder, CO). The power density was 274 W/cm$^2$ at the sample site.

After spectral analyses and photography, the tissue samples were fixed in 10% phosphate buffered formalin. The tissues were dehydrated in graded ethanol solution and xylene, and embedded in paraffin. Each of the lesions was sectioned at 5 μm. The sections were stained with Gill's hematoxylin eosin and picrosirius red F3BA stains. The specimens stained with picrosirius red F3BA were observed with a polarizing microscope (Reichert, Veins, Austria). The other specimens were observed with a normal optical microscope (Vanox-T, Olympus, Japan). Both microscopes were equipped with a color video camera with 3 CCD chips (DXC-97 MD, Sony, Japan) for obtaining histologic images.

## RESULTS

After argon laser treatment, the tissue surface ($x$-$y$ plane) became distorted and curved to form a meniscus as shown in Figure 1. The white light illuminated photograph and the native fluorescence image of the laser-induced thermally la-

**TABLE 1. Diameter (mm) of Thermal Damage Regions (x–y) Irradiated for Different Times at a Power Density of 274 W/cm$^2$ Measured by Native Fluorescence Imaging and Photography**

| | Time (sec) | | | | |
|---|---|---|---|---|---|
| Method | 3 | 6 | 9 | 12 | 15 |
| Fluorescence imaging (mm) | 1.40 ± 0.04 | 1.84 ± 0.03 | 1.95 ± 0.04 | 2.39 ± 0.17 | 2.81 ± 0.04 |
| Photography (mm) | 1.09 ± 0.02* | 1.79 ± 0.03 | 1.89 ± 0.05 | 2.51 ± 0.12 | 2.94 ± 0.02 |

*$P < 0.01$.

ser damaged tendon sample surfaces are shown in Figure 4a and b, respectively. The corresponding *y-z* plane section images from the tissue are shown in Figure 5. Native collagen fluorescence decreases in the laser-induced tissue. The fluorescence images in Figures 4b and 5b clearly show the thermal region. The thermal damage region becomes darkened in the fluorescence image that corresponds to a decrease in the collagen fluorescence at 380 nm. A narrow zone of gradual fluorescence loss can be seen between the normal and the thermally damaged area. The boundary line (Fig. 4b) is easy to identify. The thermally damaged region on the native fluorescence imaging (Figs. 4b, 5b) is much clearer than that of the white light photography. The apparent difference in the upper boundary of the white light and fluorescence images for *y-z* plane section is due to the visibility of the meniscus wall in the white light photograph (see Fig. 5a). In the fluorescence image (see Fig. 5b), the meniscus wall became invisible due to the absence of collagen fluorescence from this region.

The diameters of the thermal damage regions on the surface (*x-y* plane), measured from the native fluorescence images and the white light photographs are listed in Table 1 as a function of laser exposure. There is a statistical difference between the fluorescence images and the white light photographs ($F = 10.30497$, $P = 0.00933$) measured from the 3-second irradiation group.

Figure 6 shows histologic *y-z* plane sections of the samples. The slide stained with picrosirius red F3BA without polarized light is shown in Figure 6a. Some tissue structures disappeared in the laser-treated region and became homogenized after laser irradiation. The junction between normal and thermally damaged tissues is not evident. The same slide illuminated with polarized light is shown in Figure 6b. The normal collagen fibers, which were not in the laser treated area, appear yellow/orange. The collagen in the thermally damaged region denatured, resulting in a

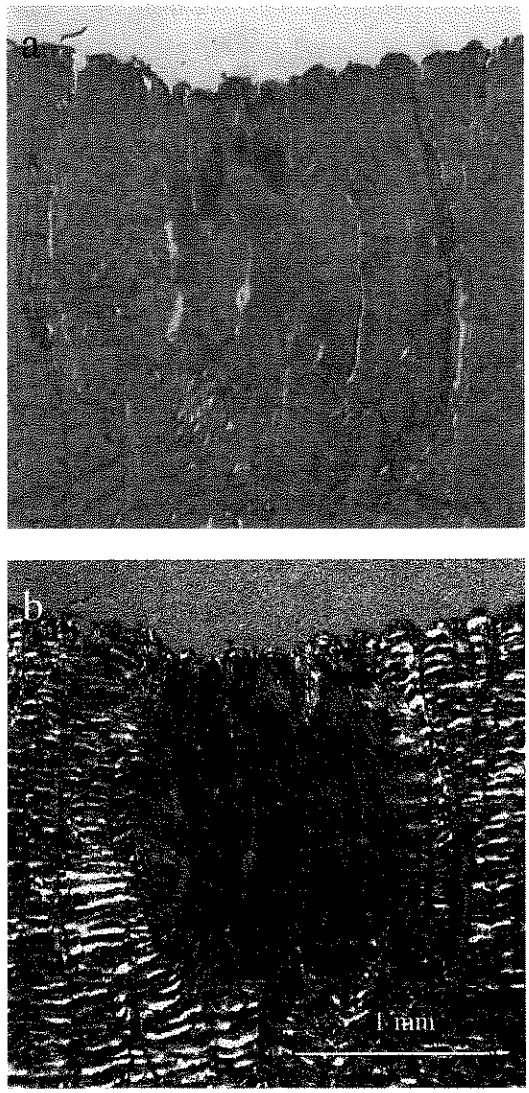


Fig. 6. Histologic *y-z* plane section of a tendon tissue sample after laser irradiation. **a:** Section is stained by using picrosirius red F3BA without polarized light. The tissue structure in the center of the thermal damage region disappears and becomes homogenized. The junction between the normal and the thermally damaged tissues cannot be identified. **b:** Under polarized light, stained collagen fibers appear yellow/orange. The thermally damaged region shows a loss of collagen's natural birefringence and appears darkened (original magnification, ×18. Scale bar applies to a,b.

**TABLE 2. Depth (mm) of Thermal Damage Regions (y–z) Irradiated for Different Times at a Power Density of 274 W/cm$^2$ Measured by Native Fluorescence Imaging, Histology, and Photography**

| | Time (sec) | | | | |
|---|---|---|---|---|---|
| Method | 3 | 6 | 9 | 12 | 15 |
| Fluorescence imaging (mm) | 1.07 ± 0.23 | 1.57 ± 0.12 | 1.68 ± 0.23 | 1.82 ± 0.39 | 2.13 ± 0.28 |
| Histology (mm) | 1.05 ± 0.15 | 1.52 ± 0.22 | 1.70 ± 0.34 | 1.80 ± 0.27 | 2.15 ± 0.31 |
| Photography (mm) | 0.82 ± 0.23* | 1.61 ± 0.15 | 1.63 ± 0.17 | 1.77 ± 0.34 | 2.08 ± 0.29 |

*$P < 0.05$.

loss of its natural birefringence. This region clearly became very discolored and darkened. The thermal damage region in this slide is similar to that shown in the native fluorescence image (Fig. 5b). Both images show stronger thermal damage on the laser irradiated tissue region in the center of the damaged region and much less on the surface. After a tissue-shrinkage correction factor of 1.15 is multiplied [10,11], the maximal depth of the thermal damage region were measured on the slides stained with picrosirius red F3BA and illuminated with polarized light. The maximal depths (see Fig. 1) of the thermal damage region on the *y-z* plane sections measured from the native fluorescence images, histology, and white light photograph in each group are listed in Table 2. There is a difference between the fluorescence image and the white light photograph ($F = 3.5974$, $P = 0.03158$) in the 3-second irradiation group.

## DISCUSSION

The emission from collagen in a laser treated tissue area is reduced in comparison to the surrounding tissue region. The changes are confirmed by histology with picrosirius red F3BA stain observed under a polarizing microscope. Collagen denatures at approximately 65°C [12]. The regional demarcation of native fluorescence is the basis for the quantitative nature of the technique. The spatial extent of native fluorescence image is similar to the region measured by histology. Both methods show that the greatest thermal damage occurs in the center of the region, not at the surface of tissue. Little thermal damage on the surface tissue may be due to cooling to the ambient room temperature. The depths of the thermal damage regions, which are observed from the fluorescence image and histology, are similar.

Although a variety of changes may be apparent on the white light illuminated photography [13], as shown in Figures 4a and 5a, the border between normal and damaged tissue is not clear. Especially when the examined tissue is a light pigment one, the identification becomes very difficult. Our study shows that there is an underestimate in the detection of small (≥1 mm) thermal damage regions at short exposure times, such as in the 3-second irradiation group, when examined by the naked eye (photography, see Tables 1 and 2).

The histology with picrosirius red F3BA stain, as a specific stain for the collagen molecule, illuminated by polarized light has confirmed the reduction of collagen in the fluorescence image. The sulphonic acid groups of the dye react with basic groups on the collagen molecule, the natural birefringence of collagen being then enhanced by the parallel relationship of the elongated dye molecules [13]. Thermally denatured collagen does not exhibit this birefringence. The collagen fibers may become merged into an amorphous random state. Therefore, collagen denaturation can be used as a marker for thermal damage in histology [14]. This method has been used to examine the effect of laser energy on collagen in vascular tissue thermal damage [14,15].

Native fluorescence from tissue allows for in situ local imaging of collagen distribution in tissue. Native fluorescence imaging can be used as a noninvasive diagnostic tool for investigating laser irradiation in in vitro tissue examination. This study shows the changes in the collagen state from native fluorescence imaging for detecting thermal damage in tissues. Native fluorescence demonstrates the molecular changes in tissue after heat treatment. Native fluorescence imaging showing a thermal damage region is more sensitive and clearer than the method of light illuminated photography. The latter only depends on tissue color changes. With this approach, it may become possible to evaluate in vivo laser treatments for laser photocoagulation, interstitial hyperthemia, plastic surgery, and welding.

## ACKNOWLEDGMENTS

The authors thank Dr. B. Xu for operating the argon laser and Drs. N. Ockman and J. Evans for reviewing the manuscript.

## REFERENCES

1. Thomsen S. Pathologic analysis of photothermal and photomechanical effects of laser-tissue interaction. Photochem Photobiol 1991;53:825–835.
2. Barbeau GR, Abela GS, Seeger JM, Friedl SE, Tomaru T, Giacomino PP. Temperature monitoring during peripheral thermo-optical laser recanalization in humans. Clin Cardiol 1990;13:690–697.
3. Badeau AF, Lee CE, Morris JR, Thompson S, Malk EG, Welch AJ. Temperature response during microvascular anastomosis using milliwatt $CO_2$ laser. Lasers Surg Med 1986;6(Suppl):179.
4. Maitinot VJ, Mordon SR, Mitchell VA, Pellerin PN, Brunetaud JM. Determination of efficient parameters for argon laser-assisted anastomoses in rats: macroscopic, thermal, and histological evaluation. Lasers Surg Med 1994;15:168–175.
5. Bass LS. Laser tissue welding: a comprehensive review of current and future clinical applications. Lasers Surg Med 1995;17:315–349.
6. Alfano RR, Tata DB, Cordero J, Tomashefsky P, Longo FW, Alfano MA. Laser induced fluorescence spectroscopy from native cancerous and normal tissue. IEEE J Quant Electronics 1984;20:1507–1511.
7. Tang J, Zeng F, Savage H, Ho PP, Alfano RR. Fluorescence spectroscopic imaging to detect changes in collagen and elastin following laser tissue welding. J Clin Laser Med Surg 2000;18:3–7.
8. Nimni ME. Collagen, structure and function. In: Dulbecco R, editor. Encyclopedia of human biology, vol 2, 2nd ed. New York: Academic Press; 1997. p 877–895.
9. Rucker RB, Tinker D. Elastin. In: Dulbecco R, editor. Encyclopedia of human biology, vol 3, 2nd ed. New York: Academic Press; 1997. p 573–582.
10. Boonstra H, Oosterhuis JW, Oosterhuis AM, Fleuren GJ. Cervical tissue shrinkage by formaldehyde fixation, paraffin wax embedding, section cutting and mounting. Virchows Arch A Pathol Anat Histopathol 1983;402:195–201.
11. Schned AR, Wheeler KJ, Hodorowski CA, Heaney JA, Ernstoff MS, Amdur RJ, Harris RD. Tissue-shrinkage correction factor in the calculation of prostate cancer volume. Am J Surg Pathol 1996;20:1501–1506.
12. Lelons M, Flandin F, Herbage D, Allain J-C. Influence of collagen denaturation on the chemorhelogical properties of skin assessed by differential scanning calorimetry and hydrothermal isometric tension measurements. Biochem Biophys Acta 1982;717:295–300.
13. Boulnois J-L. Photophysical processes in recent medical laser developments: a review. Lasers Med Sci 1985;1:47–66.
14. Brooks SG, Ashley S, Wright S, Davies GA, Kester RC, Rees MR. The histological measurement of laser-induced thermal damage in vascular tissue using the stain picrosirius red F3BA. Lasers Med Sci 1991;6:399–405.
15. Macruz R, Ribeiro MP, Brum JMC. Laser surgery in enclosed spaces: a review. Lasers Surg Med 1985;5:199–218.